COMMUNICATION

Self-delivery of N-hydroxylethyl Peptide Assemblies to the Cytosol Inducing Cancer Cell Endoplasmic Reticulum Dilation

Received 00th January 20xx,
Accepted 00th January 20xx

DOI: 10.1039/x0xx00000x

Shijin Zhang,[a] Xunwu Hu,[a] Dingze Mang,[a] Toshio Sasaki [b] and Ye Zhang*[a]

Inspired by clinical studies on alcohol abuse induced endoplasmic reticulum disruption, we designed *N*-hydroxylethyl peptide assembly to regulate ER stress response in cancer cell. Coupling with coumarin derivative via ester link, a prodrug was synthesized to promote esterase-facilitated self-delivery of *N*-hydroxylethyl peptide assemblies around ER inducing ER dilation. Following that, ER-specific apoptosis was effectively and efficiently activated in various types of cancer cells including the drug resistant and metastatic ones.

Endoplasmic reticulum (ER) is an elaborate network membrane that extends throughout the cell. Via membrane contacts, ER communicates with mitochondria, Golgi, endosomes, peroxisomes, lipid droplets, and the plasma membrane (PM) for coordination activities which is essential for cell homeostasis.[1] Although the underlying mechanism is still elusive, the importance of ER in the control of cell fate makes it one of the major targets for therapeutic research. At present, several natural products have shown potentials in regulating ER stress in various cancer cell lines by targeting key proteins of signaling pathways.[2] To improve therapeutic efficiency, more investigation and preclinical feedbacks to modify the molecular approach is highly demanded.

In clinical studies, elevated ER stress is commonly detected in alcoholic patients. The ER stress following chronic alcohol abuse contributes to damage and dysfunction in liver, pancreas, heart, and brain. For example, ER dilation occurs in hepatocytes of alcoholics which is associated with alcoholic liver disease.[3] Despite all the health risks, scientists made an interesting discovery that under the treatment of alcohol, the unfolded protein response (UPR) could be activated in cancer cells causing ER stress induced cell death.[4] Although the underlying mechanism of alcohol abuse induced ER stress in cancer cell is not clear yet, the phenomenon itself is interesting, and it inspires us to create a prodrug approach to deliver alcohol derivatives reaching ER for stress regulation in cancer treatment.

To create an environment of massive accumulation of alcohol derivatives around the ER as the mimic of 'acute alcohol abuse' in cancerous cell, we designed and synthesized a *N*-hydroxylethyl peptide for cytosolic self-assembly. To achieve efficient intracellular absorption, a prodrug designed to promote the self-delivery[5] mediated by carboxylesterase (CES)[6-9] was introduced (Figure 1).

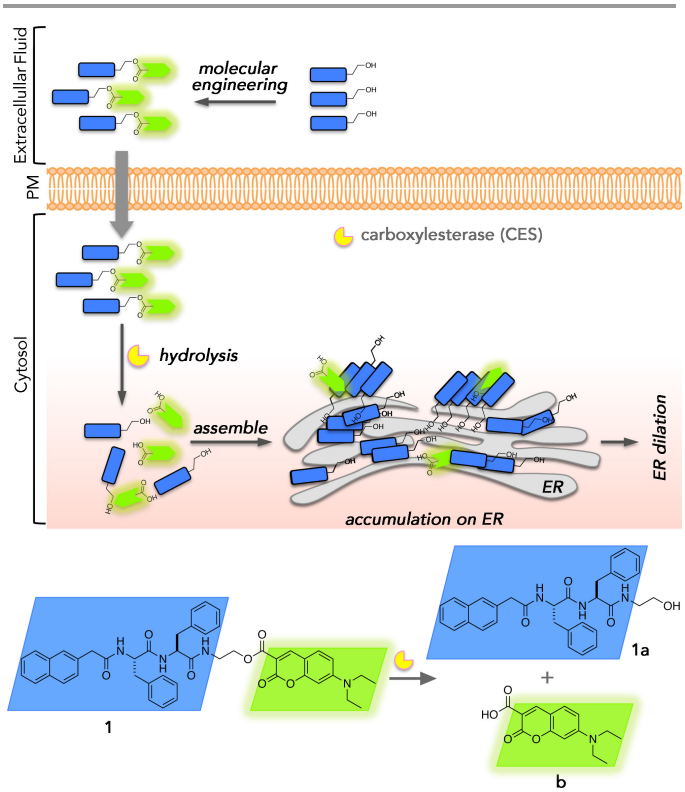

Figure 1. Schematic illustration of *N*-hydroxylethyl peptide 1a assembly induced ER dilation, and the prodrug design to promote 1a intracellular absorption via CES-catalyzed hydrolysis.

[a] *Bioinspired Soft Matter Unit, Okinawa Institute of Science and Technology Graduate University (OIST), 1919-1 Tancha, Onna son, Okinawa, 904-0495 Japan.*
[b] *Imaging Section, Okinawa Institute of Science and Technology Graduate University (OIST), 1919-1 Tancha, Onna son, Okinawa, 904-0495 Japan Address here.*

Electronic Supplementary Information (ESI) available: [molecular synthesis, physical characterizations, and biological protocols]. See DOI: 10.1039/x0xx00000x

To minimize the structure modification induced functional alterations, we selected a super small molecular hydrogelator, Naphthalene-Phe-Phe,[10] as the self-assembly building block to couple with ethanolamine for the alcohol derivative **1a**. The hydroxyl group of **1a** was protected by fluorescent coumarin derivative **b** via an ester link to obtain the prodrug **1**. To prove that the design is rational and practical, two molecules **2** and **3** were synthesized and characterized in comparison to **1** (Scheme 1). Under the treatment of CES, **1** was hydrolyzed to **1a** and **b** (Figure S1, S2a-c), **2** was hydrolyzed to **2a** and **b** (Figure S1, S2d-f). Without ester linkers, molecule **3** couldn't be hydrolyzed by CES (Figure S1).

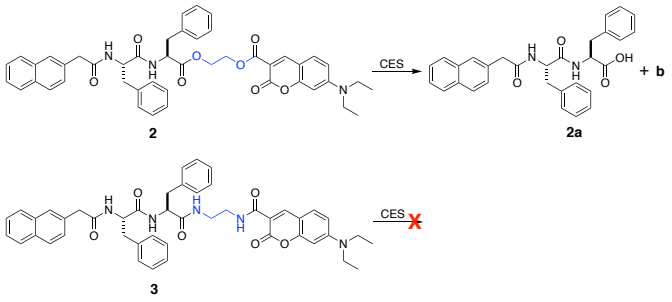

Scheme 1. CES-catalyzed hydrolysis of **2** and **3**. Reaction conditions: borate buffer, pH = 8.0, 37 °C.

The lipophilicity of a molecule (lipid-water partition coefficient log*P*) is a crucial factor governing passive diffusion. Therefore, we characterized $\log P_{oct/wat}$ of all three molecules by testing their distribution in a two-phase octanol/water system (Figure S3), and the results were summarized in Figure 2A. Considering the $\log P_{oct/wat}$ that results in the maximum rate of diffusional transport through biological membranes generally has a value of about 2,[11, 12] **1** and **3** are close to optimal lipophilicity compare with molecule **2**. Since molecules **1**, **2** and **3** all self-assemble over certain concentrations, we evaluate their ability of self-assembly using transmission electron microscopy (TEM). By comparing the critical concentrations for self-assembly and for forming stabilized nanostructures (Figure S4), we found that the order of self-assembly ability was **3** > **2** > **1**. In borate solution of **1** (125 μM), the addition of CES induced transition of self-assembled structure from sparse aggregates to uniformed nanofibers (Figure 2B). For the borate solution of **2**, CES disassembled dense nanovesicles into scattered aggregates (Figure 2C). Self-assembled dense nanofibers of **3** was intact after the addition of CES (Figure 2D). Apparently, **1** is a promising prodrug candidate with relatively optimal lipophilicity and CES-hydrolysis-enhanced assembly leading to stabilized cytosolic drug accumulation.

At various concentrations, the circular dichroism (CD) spectra of **1a**/**b** or **2a**/**b** mixture were different from the simple sums of their individual CD spectra (Figure 2E and Figure S5) suggesting that hydrolyzed components **1a** and **b**, or **2a** and **b** would co-assemble in cytosol resulting into fluorescent nanostructures (Figure 2F).[13] Under the confocal microscope, HeLa cells cultured with **1** or **2**, co-stained on plasma membrane using CellMask green showed strong fluorescence solely in cytosol implying efficient cell penetrations (Figure 2G, 2H and S6). **3** was hardly absorbed by HeLa cells, instead, molecular assemblies were observed outside of cells attached to the culture dish (Figure 2I). The enzyme-catalyzed hydrolysis of **1** and **2** in HeLa cell lysate and extracellular culture medium indicated that the hydrolysis only occurred inside HeLa cells (Figure 2J). Therefore, we evaluated molecular absorption efficiency by quantifying the remaining molecules in extracellular culture medium of cultured HeLa cells under the treatment of molecules at low concentration for short period without causing cell death induced release of molecules. Figure 2K indicated that **1** and **2** had more than seven times higher absorption rate than **1a** and **2a** implicating the prodrug design effectively promoted the cell absorption.

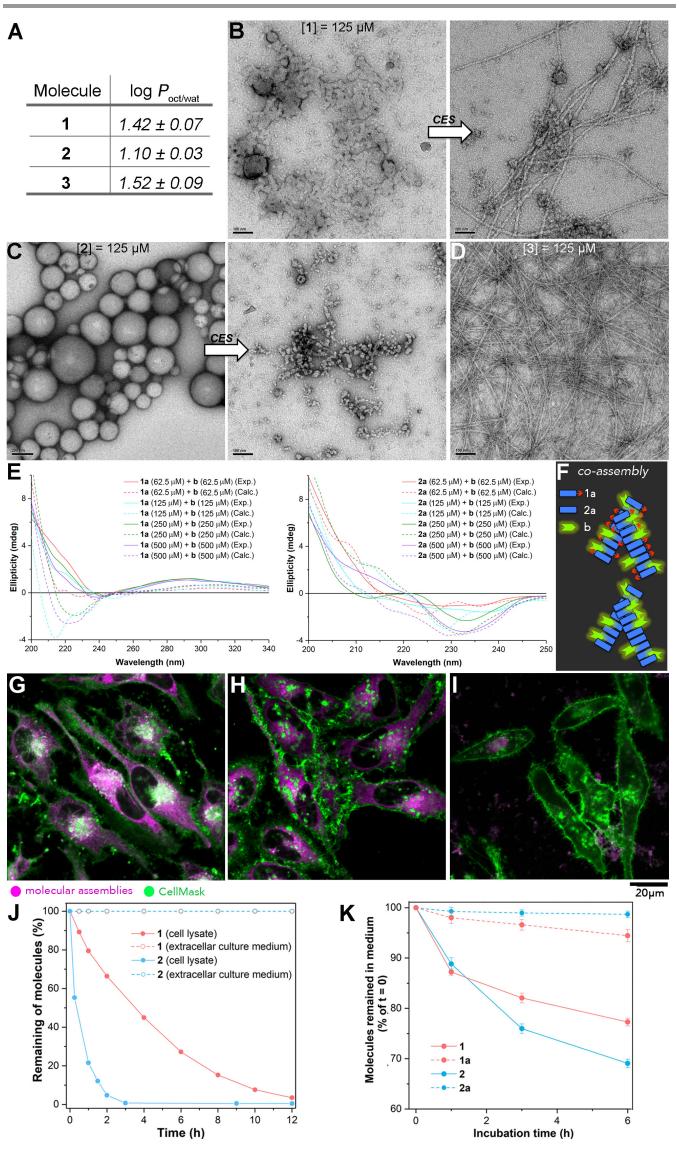

Figure 2. (A) A table of lipid-water partition coefficients of molecules 1, 2 and 3. TEM images of molecule 1 (B), 2 (C) in borate butter at a concentration of 125 μM before (left) and after (right) the CES-catalyzed hydrolysis. The scale bars represent 100 nm. (D) TEM image of molecule 3 (125 μM) in borate buffer. (E) CD spectra of 1a/b (1:1) mixtures (left) and 2a/b (1:1) mixtures (right) at various concentrations. Exp. and Calc. represent experimental and theoretically calculated CD spectra, respectively. (F) Schematic illustration of molecular co-assembly between 1a and b or between 2a and b. Fluorescent images of HeLa cells incubated with 1 (G), 2 (H), or 3 (I) at concentration

of 10 μM for 4 hours and stained with CellMask Green (plasma membrane). Violet represents the emissions of coumarin derivatives. The scale bar represents 20 μm. (J) Kinetic profiles of CES-catalyzed hydrolysis of 1 or 2 in HeLa cell lysate or extracellular culture medium (isolated from cultured cells) at 37 °C. (K) Relative percentage of 1, 1a, 2, or 2a remained in extracellular culture medium during the first 6-hour HeLa cell incubation under the treatment of those molecules at concentration of 10 μM.

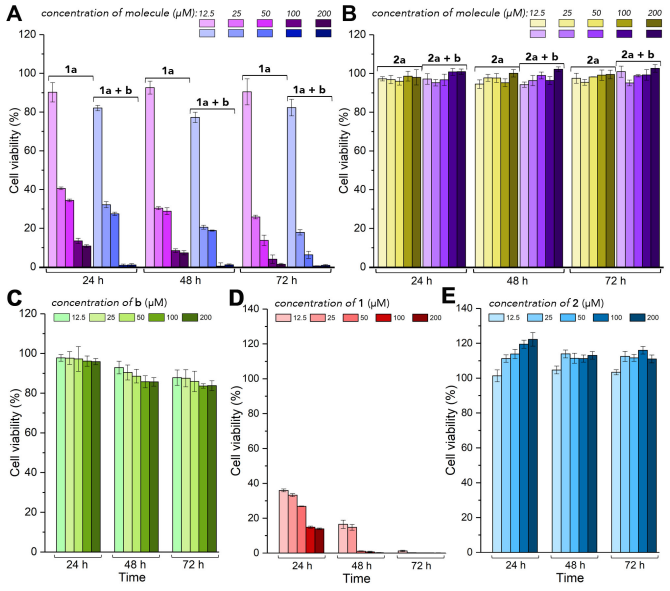

Figure 3. HeLa cell viability under the treatment of 1a and 1a/b mixture (1:1) (A), 2a or 2a/b mixture (1:1) (B), b (C), 1 (D), and 2 (E) at various concentrations.

HeLa cell viability results indicated that **1a** was toxic (Figure 3A), while **2a** was biocompatible (Figure 3B) at various concentrations. Apparently, the structure modification of alcohol molecule into **1a** successfully maintained the toxicity. The protection building block **b** barely showed toxicity on HeLa cells (Figure 3C). As a combination of effects from individual components, the **1a**/**b** mixture showed slightly higher toxicity than **1a** (Figure 3A), while **2a**/**b** mixture diluted the toxicity of **b** causing biocompatibility (Figure 3B). The results suggested that co-assembly with **b** didn't affect the overall toxicity of **1a** and **2a**. Compare with **1a** and **2a**, **1** exhibited the highest toxicity on HeLa cells (Figure 3D) and molecule **2**, in contrast, was biocompatible (Figure 3E) implying the success of prodrug design by promoting the cell uptake without affecting the cytotoxicity of **1a** and **2a**.

High-resolution confocal imaging showed that following the treatment of **1**, **1a**/**b** co-assemblies occupied HeLa cell cytosol surrounding ER and mitochondria without obvious co-localization implicating possible close contacts (Figure 4A). Compare with the rough ER in untreated HeLa cells (Figure 4B), molecule **1** caused severe ER dilation (Figure 4C).[14] Molecule **2**, in contrast, did not cause ER dilation (Figure 4D). The structure of mitochondria was not affected by the treatment of **1** or **2**. To elucidate the correlation between molecule **1** induced ER abnormality and HeLa cell death, we evaluated the time-dependent apoptosis activation under the treatment of **1** by western blotting (Figure 4E). The expression of cleaved Caspase-9 showed no obvious changes during the first 12-hour incubation. Only after 24-hour treatment, with low HeLa cell viability (Figure 3D), it increased to 3 times higher than the control implicating that the apoptosis was not directly triggered by mitochondria disruption or dysfunction (Figure 4F),[15] which is consistent with their intact morphology in TEM images (Figure 4C). The expression of cleaved Caspase-12 dramatically increased over time (Figure 4G) confirming ER-specific apoptosis was activated.[16] Besides structural disruption, accumulation of unfolded proteins also results in ER stress.[17] Following the persistent ER stress, opposing UPR signals converge on DR 5 and engage the apoptosis via Caspase-8.[18] Neither the expression of DR 5 (Figure 4H) nor cleaved Caspase-8 (Figure 4I) showed obvious increment. Therefore, under the treatment of **1**, the ER-specific apoptosis was mainly induced by ER structure disruption–ER dilation.

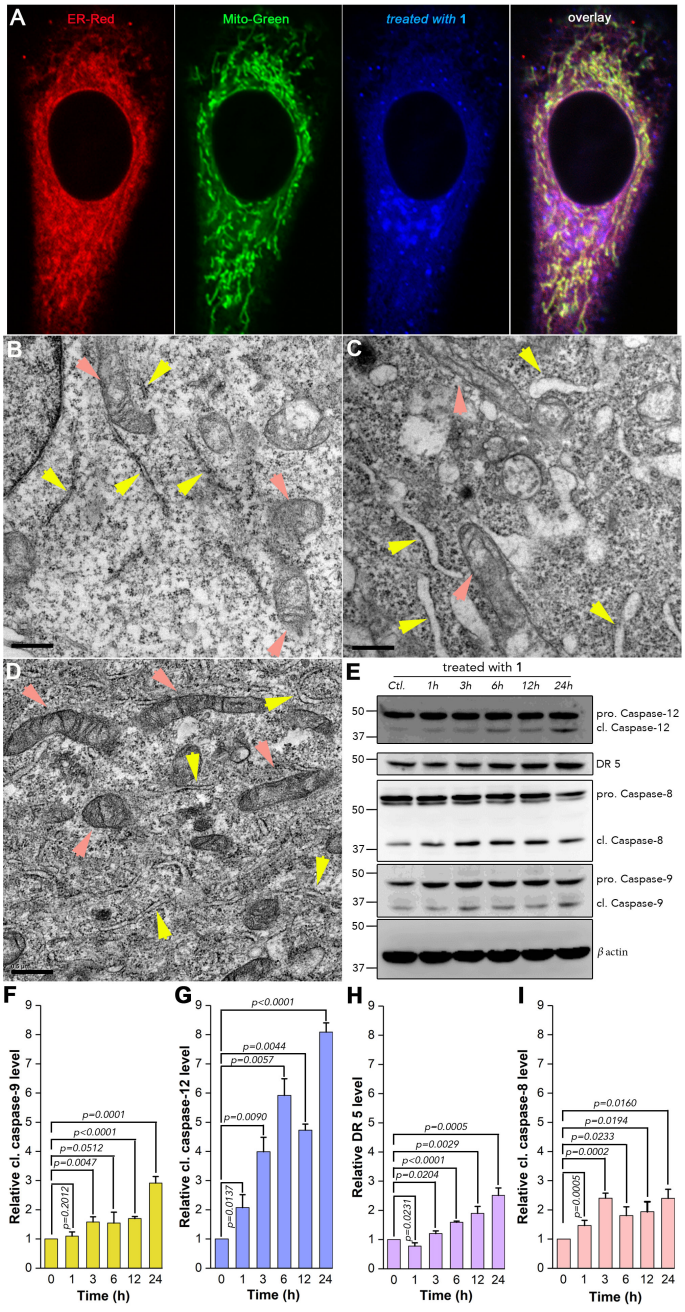

Figure 4. (A) Fluorescence HeLa cell images after incubating with 1 (10 μM) for 4 hours and co-stained with ER-Red, Mito-Green. Blue represents the emissions of molecule 1's derivatives. TEM images of HeLa cell without treatment (B), under the treatment of 1 (C) or under the treatment of 2 (D). The ER was marked by yellow arrowhead. The mitochondria were marked by pink arrowheads. (E) Western blotting for Caspase-12, DR 5, Caspase-8, and Caspase-9 expressed in HeLa cells under the treatment of 1 (20 μM). *β* actin is the loading control. Time-dependent relative expression profiles of cl. Caspase-9 (F), cl. Caspase-12 (G), DR 5 (H), and cl. Caspase-8 (I). Results are means ± S.D. of three independent experiments.

Various cancer cell lines including ovarian cancer (SKOV3 and drug resistant OVCAR-3), liver cancer (HepG2), and metastatic pancreatic cancer (PANC-1) were applied to evaluate the anticancer efficacy of the prodrug **1**. The cell viability results clearly implicated anticancer effect (Figure 5). One-day treatment of **1** at 12.5 μM concentration killed more than 40% of all four types of cancer cells. Using 12.5, 25, 50, and 200 μM of **1**, around 90% of SKOV3, OVCAR-3, HepG2 and PANC-1 cells were killed in two days, respectively.

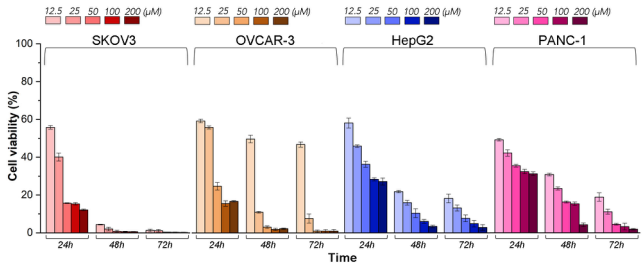

Figure 5. SKOV-3, OVCAR-3, HepG2 and PANC-1 cell viability under the treatment of **1** at various concentrations.

Conclusions

Clinical studies on alcohol abuse induced ER stress provided the fundamental information that stimulated the design of *N*-hydroxylethyl peptide **1a** for cancer treatment via intracellular molecular-assembly inducing accumulation of alcohol derivatives as a mimic of 'acute alcohol abuse'-like condition of ER. Facilitated by CES, prodrug **1** promotes self-delivery of **1a** and activated ER-specific apoptosis efficiently. Besides the development of potential anticancer drug and prodrug, the study of synthetic molecular assembly induced ER dilation will contribute to studies on specific importance of the ER stress response in cancer cells and thus provides promising strategies for ER-targeted therapeutic applications.

Conflicts of interest

There are no conflicts to declare.

Acknowledgement

The author would like to thank Toshiaki Mochizuki who is a technician of imaging section of OIST for his help in confocal imaging and western blotting. The research is supported by Okinawa Institute of Science and Technology Graduate University (OIST), Proof of Concept (POC) Programm from R&D Section of OIST, and Takeda Science Foundation for medical research.

Notes and references

1. H. X. Wu, P. Carvalho and G. K. Voeltz, *Science*, 2018, **361**, Cp15-U70.
2. A. A. Farooqi, K. T. Li, S. Fayyaz, Y. T. Chang, M. Ismail, C. C. Liaw, S. S. F. Yuan, J. Y. Tang and H. W. Chang, *Tumor Biol*, 2015, **36**, 5743-5752.
3. B. P. Lane and C. S. Lieber, *Am J Pathol*, 1966, **49**, 593-&.
4. D. L. Howarth, A. M. Vacaru, O. Tsedensodnom, E. Mormone, N. Nieto, L. M. Costantini, E. L. Snapp and K. C. Sadler, *Alcohol Clin Exp Res*, 2012, **36**, 14-23.
5. S. Y. Qin, A. Q. Zhang, S. X. Cheng, L. Rong and X. Z. Zhang, *Biomaterials*, 2017, **112**, 234-247.
6. S. C. Laizure, V. Herring, Z. Y. Hu, K. Witbrodt and R. B. Parker, *Pharmacotherapy*, 2013, **33**, 210-222.
7. F. M. Williams, *Clin Pharmacokinet*, 1985, **10**, 392-403.
8. Z. Q. Q. Feng, H. M. Wang, R. Zhou, J. Li and B. Xu, *J Am Chem Soc*, 2017, **139**, 3950-3953.
9. B. C. Yu, Y. Q. Zheng, Z. N. Yuan, S. S. Li, H. Zhu, L. K. De la Cruz, J. Zhang, K. L. Ji, S. M. Wang and B. H. Wang, *J Am Chem Soc*, 2018, **140**, 30-33.
10. Y. Zhang, Y. Kuang, Y. A. Gao and B. Xu, *Langmuir*, 2011, **27**, 529-537.
11. Miles Hacker, Kenneth Bachmann and W. Messer, *Pharmacology: Principles and Practice*, ELSEVIER, 2009.
12. D. G. Watson, *Pharmaceutical Chemistry*, ELSEVIER, 2011.
13. W. Ji, S. J. Zhang, G. A. Filonenko, G. Y. Li, T. Sasaki, C. L. Feng and Y. Zhang, *Chem Commun*, 2017, **53**, 4702-4705.
14. M. Akiyama, M. Hatanaka, Y. Ohta, K. Ueda, A. Yanai, Y. Uehara, K. Tanabe, M. Tsuru, M. Miyazaki, S. Saeki, T. Saito, K. Shinoda, Y. Oka and Y. Tanizawa, *Diabetologia*, 2009, **52**, 653-663.
15. C. Guegn, M. Vila, G. Rosoklija, A. P. Hays and S. Przedborski, *J Neurosci*, 2001, **21**, 6569-6576.
16. T. Nakagawa, H. Zhu, N. Morishima, E. Li, J. Xu, B. A. Yankner and J. Y. Yuan, *Nature*, 2000, **403**, 98-103.
17. C. Hetz, *Nat Rev Mol Cell Bio*, 2012, **13**, 89-102.
18. M. Lu, D. A. Lawrence, S. Marsters, D. Acosta-Alvear, P. Kimmig, A. S. Mendez, A. W. Paton, J. C. Paton, P. Walter and A. Ashkenazi, *Science*, 2014, **345**, 98-101.

1